Materials Advances

ROYAL SOCIETY OF CHEMISTRY

REVIEW

View Article Online
View Journal | View Issue

Cite this: *Mater. Adv.*, 2021, 2, 2892

Emergent 2D materials for combating infectious diseases: the potential of MXenes and MXene–graphene composites to fight against pandemics

Neeraj Dwivedi, *[ab] Chetna Dhand,[ab] Pradip Kumar[ab] and A. K. Srivastava*[ab]

Infectious diseases spread rapidly among humans, and they are amid the major causes of human deaths globally. The world has seen several fatal infectious diseases in the past, for example, Spanish flu about a century ago, and now coronavirus disease-19 (COVID-19), the two major pandemics. While medicines and vaccines are the ultimate solutions to combat pandemics, material innovation and technological development are also crucial parts to fight against these highly infectious diseases. Materials and technological development can assist in developing high-performance and sensitive diagnostic devices, efficient antimicrobial components/personal protective equipment such as face masks and shields, aprons, sterilizers, touch-free components for sanitizations, and many other components for medical equipment. Due to the outstanding functional properties and feasibility to integrate with any systems, 2D materials are emerging solutions for biomedical applications. In particular, 2D materials beyond graphene such as MXenes, and composites of MXene–graphene show many promising properties such as high electrical conductivity, surface functionalization feasibility, excellent photocatalytic and photo-to-heat conversion properties, outstanding antimicrobial behavior, and many other tailorable properties. Here, we shed light on the properties of MXenes and MXene–graphene composites for healthcare applications and how they can contribute in the fight against the current and future pandemics.

Received 4th January 2021,
Accepted 17th March 2021

DOI: 10.1039/d1ma00003a

rsc.li/materials-advances

1. Introduction

The earliest pandemic happened during 430 BC in Greece, which was suspected due to typhoid disease.[1] Since then, the world has witnessed several pandemics over the years, namely, the Antonine Plague and the Plague of Cyprian (165 AD and 250 AD), leprosy (11th century), the Black Death (1350), the Columbian exchange (1492), the Great Plague of London (1665), the first cholera pandemic (1815), the third plague pandemic (1855), Fiji measles pandemic (1875), the Russian flu (1889), the Spanish flu (1918), the Asian flu (1957), human immunodeficiency virus infection/acquired immune deficiency syndrome (HIV/AIDS, 1981), severe acute respiratory syndrome (SARS, 2003), and the most recent novel corona virus disease 2019 (COVID-19).[1] These pandemics have caused huge human losses and destroyed the economy massively. What could be learnt from these pandemics is that the technology, materials, vaccines, and medicines together are crucial to control the disease spread, treat the patients and minimize human mortality. This is how improved technologies, materials, medicine knowledge, *etc.*, have controlled the COVID-19 pandemic fatality rate to a great extent so far, and the development of effective vaccines and medicines is under progress in an unbelievable pace. Nonetheless, the discovery of novel materials and technologies in a regular interval for cross-disciplinary applications is always required to improve the capability of fighting pandemics.

Material innovation plays a vital role in new technological development. In particular, 2D materials have attracted huge attention in biomedical science and technology in the recent past.[2–4] Graphene and related 2D materials show high electrical mobility and conductivity, high surface area, excellent antiviral and antibacterial properties, photothermal and photocatalytic properties, electromagnetic shielding properties, sensing and detection, their surfaces can be functionalized with various functional groups, and they can be integrated with emerging manufacturing technologies such as additive manufacturing.[5–17] These characteristics enable them to be deployed directly or indirectly in various biomedical systems. Recent works showed the development of several components based on graphene and its derivatives to fight against COVID-19.[4,18–21] In particular, graphene-/graphene-composite-based antiviral coatings, diagnosis devices, face masks, 3D-printed medical components, gloves,

[a] *CSIR-Advanced Materials and Processes Research Institute, Bhopal-462026, India. E-mail: neeraj.dwivedi@ampri.res.in, neerajdwivedi6@gmail.com, director@ampri.res.in*
[b] *Academy of Scientific and Innovative Research (AcSIR), CSIR-Advanced Materials and Processes Research Institute, Bhopal-462026, India*

sterilizers, *etc.*, have been developed in a span of very short time-period.[4,18–21]

MXenes and related materials are another important class of 2D materials, which display astonishing physicochemical and biomedical properties, and have attracted considerable scientific and technological attention.[22] Specifically, MXenes display excellent antibacterial behavior, light-to-heat conversion and photocatalytic efficacies, and high electrical conductivity, and can contain functional groups depending upon the application.[22–25] These properties enable their potent applications in biomedical systems. Importantly, when joined together, the MXene–graphene composite shows promising properties due to synergistic effects. This has been proved for various applications, for example, MXene–graphene composites have been utilized for the development of high-performance wearable strain sensors,[26] electrically and thermally conductive composite materials,[27–29] electromagnetic interface shielding materials[30] and energy storage systems,[31,32] and their performance is expected to be excellent for biomedical applications as well. Similarly, the introduction of MXenes into the matrix of various other materials or *vice versa* has also led to an enhancement of the properties.[33–35] In view of this, MXene composites also have huge potential for biomedical applications, including for combating current and futuristic pandemics.

In this review, we discuss in detail the potential of emerging 2D materials such as MXenes and MXene-based composites to combat COVID-19 and future pandemics.

2. Emerging 2D materials and their composites: fundamentals, synthesis and properties

Graphene is a single layer of sp^2-hybridized carbon atoms arranged in a honeycomb structure, as shown in Fig. 1a.[36] Monolayer graphene exhibits excellent electronic, thermal, mechanical and optical properties. Graphene has a unique band structure, as shown in Fig. 1b.[36] The points at which the valence band and conduction band meet are called the Dirac points and electrons always move at a constant speed on all these six points. Due to a unique band structure, graphene shows ultrahigh electron mobility, for example 200 000 $cm^2\ V^{-1}\ s^{-1}$. Graphene exhibits not only excellent electronic properties, but also ultrahigh thermal conductivity ($\sim$5000 $W\ m^{-1}\ K^{-1}$), high surface area ($\sim$2600 $m^2\ g^{-1}$), and ultimate tensile strength ($\sim$1 TPa). Additionally, single-layer graphene is optically transparent, it absorbs only $\sim$2.3% of white light.[37]

Graphene was first synthesized in 2004 by a micromechanical exfoliation method.[5] In this method, monolayer graphene was achieved by peeling off graphene layers from highly orientated pyrolytic graphite using adhesive tape. This micromechanical cleavage process is well known as the "Scotch tape" method. While the Scotch tape method can produce high-quality graphene, production yield remains an issue with this method. Nevertheless, solution-based exfoliation methods were introduced for the bulk synthesis of graphene. Electrochemical exfoliation of graphite and chemical exfoliation of graphite and reduction methods were the most studied methods for bulk synthesis of graphene.

In the electrochemical exfoliation method, intercalating ions are used to exfoliate graphite.[38] This method uses anode and cathode potentials in a suitable electrolyte solution. Graphitic material is used as a working electrode. Various intercalated ions such as Li^+, Ni^{2+}, F^-, SO_4^{2-}, NO^{3-}, and Cl^- are used under different electrochemical conditions. The quality of graphene is strongly affected by the applied potential and electrolyte solution. Graphene synthesis yield can be improved by using surfactants along with ion intercalation. Graphene sheets of size up to 0.5 μm can be achieved with oxygen functional groups on its surface and edges.[39] The presence of oxygen functionalities makes the graphene sheets easily dispersible in polar and non-polar solvents. However, the electrical and thermal properties of graphene are degraded. This solvent exfoliation technique is environmentally friendly but graphene quality cannot be up to standard.

Graphene was further synthesized by chemical exfoliation and reduction methods. Modified Hummers' method is one of the well-established techniques for synthesizing highly dispersible graphene oxide.[40] The method is based on graphite flake oxidation by potassium permanganate in the presence of concentrated sulphuric acid. Fig. 2 shows the mechanism of graphene oxide synthesis.[41] First, sulphuric acid intercalates into graphite and forms graphite-intercalated compounds (GIC). After that, GIC is oxidized using $KMnO_4$ leading to the formation of graphite oxide. Oxidized graphite is converted into graphene oxide (GO) by ultrasonication, followed by centrifugation to separate the unexfoliated graphite flakes. As-obtained GO is highly soluble in aqueous and

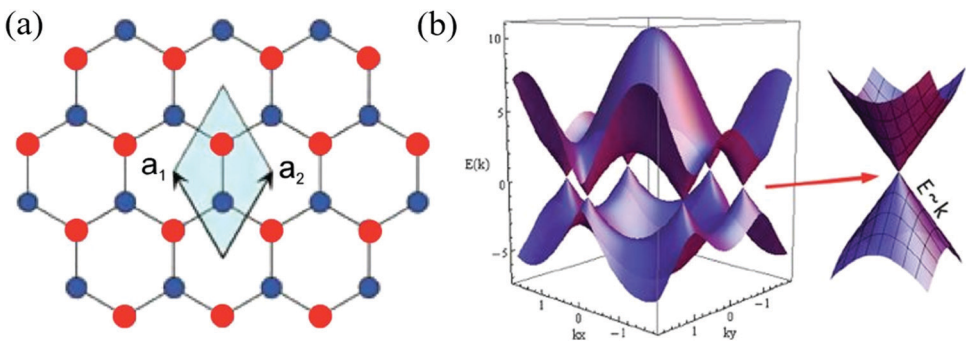

Fig. 1 Honeycomb graphene structure (a) and its band structure (b). Reproduced with permission from ref. 36.

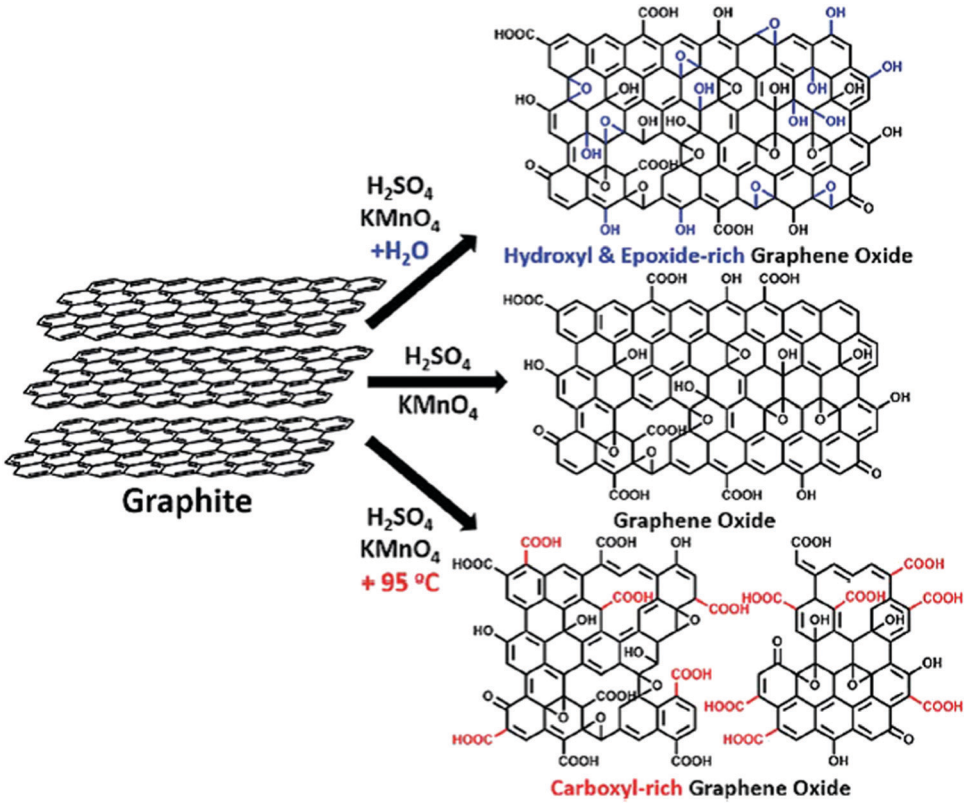

Fig. 2 Mechanism of graphite exfoliation into single-layer GO. Reproduced with permission from ref. 41.

non-aqueous solvents due to the presence of oxygen-containing functional groups on its surface and edges. This method can produce graphene oxide sheets of size in the range from 1 to 100 μm with a thickness of less than 1 nm.[42] Graphite oxidation time increases with the increase in flake size. The production yield of GO can be achieved by up to 40%, which can be further improved by up to 90% using pre-oxidized graphite flakes. GO synthesis yield up to 100% can be achieved using the K_2FeO_4 oxidation agent.[43]

The chemical oxidation and exfoliation method can produce a bulk amount of graphene oxide, but the nature of GO sheets is insulating kind due to the presence of oxygen-containing functional groups. To make it electrically conductive, oxygen-containing functional groups from GO sheets must be removed. These oxygen functionalities can be reduced by electrochemical, thermal and chemical reduction methods. The electrochemical reduction method can significantly reduce GO under ambient conditions. The C/O ratio of 3 to 10 was achieved in electrochemically reduced GO.[44] The thermal annealing method can give much better properties of reduced GO. Generally, thermal reduction of GO is performed at high temperatures (1000–2000 °C) under inert conditions. During annealing, oxygen functional groups are removed from the GO surface and, simultaneously, it is graphitized at elevated temperatures. The resultant GO powder/thin-film exhibits a very high electrical conductivity. Xin *et al.* reported the development of graphene paper *via* high-temperature (2200 °C) thermal reduction and graphitization.[45] The as-obtained free-standing graphene paper showed a high electrical conductivity of 1000 S cm^{-1} and a thermal conductivity of 1238 W m^{-1} K^{-1}. The thermal reduction method is straightforward and is being used for high-quality free-standing graphene paper and composite fabrication, but this method requires a long time for heating and graphitization. In comparison to thermal and electrochemical reductions, the GO reduction by chemical reduction method is widely employed. In this method, a chemical reaction/reduction is performed on GO film/powder at a low temperature (100 °C). In general, hydrazine hydrate is used for GO reduction in a hot aqueous solution.[46,47] Hydrazine hydrate can significantly reduce GO but the reduction mechanism is still not clear. Few other chemicals like $NaBH_4$ were also explored but reduced GO materials exhibit low electrical conductivity.[48] Furthermore, hydrohalic acids were used for the effective reduction of the GO material. For example, Kumar *et al.* reported an improved electrical conductivity of ~250 S cm^{-1} from hydriodic acid (HI)–reduced large-area graphene paper.[42] HI-reduced graphene/polymer composite films also showed high electrical and thermal conductivities of 3000 S m^{-1} and ~20 W m^{-1} K^{-1}, respectively.[49] Many other reducing agents such as lithium aluminum hydride, hydroxylamine and eco-friendly L-ascorbic acid were also used.[50] The overall performance of hydrohalic acid-reduced GO films was sufficient for practical applications.

Chemical vapor deposition (CVD) is a well-established approach for high-quality graphene in a large area. Graphene synthesis using the CVD method was first reported in 2008.[51]

In the CVD approach, copper and nickel substrates are commonly employed for graphene growth.[52,53] This method involves the decomposition of a gaseous carbon source material on a catalytic substrate at high temperatures under inert conditions. Decomposed carbon atoms are deposited on a catalytic substrate under optimized conditions. Upon growth completion, the deposited graphene layer can be transferred onto the desired substrates. CVD technique can produce single-crystal graphene sheets of size up to the centimeter scale. The quality and size of the graphene sheet mainly depend on temperature, pressure, substrate quality, and catalyst. Despite the capability of producing high-quality graphene, the CVD technique has some limitations such as post-deposition graphene transfer onto different surfaces, and removal of the metal catalyst. Moreover, the transfer process causes some structural damages, which affect the quality of graphene. The mechanism of the graphene transfer process is well described in previous studies.[54]

Besides graphene, MXenes are promising 2D materials due to their broad-spectrum properties. The MXene was first synthesized by Gogotsi and co-workers in 2011.[55] A 2D Ti_3C_2 nanosheet was produced by exfoliation of the Ti_3AlC_2 phase in hydrofluoric (HF) acid at room temperature. The 2D layered materials that are composed of transition metal carbides/nitrides are generally referred to as MXenes. More than 60 groups of layered ternary carbides and nitrides are known, which are called the MAX phases. The MAX phases are commonly represented by $M_{n+1}AX_n$ formula, where $n = 1$, 2, or 3 and M, A and X represent an early transition metal, A-group (mostly groups 13 and 14) element and C and/or N, respectively. The MAX phases have a layered hexagonal structure, as shown in Fig. 3a. The M-layers are interleaved by A group elements with X-atoms filled on octahedral sites. The group atoms are weakly bound to the structure, and can be etched out by acid treatment (Fig. 3b). Single-layer MXenes can be produced by ultrasonication of the HF-treated MAX phase (Fig. 3c). During the exfoliation process, OH and F functional groups are introduced on MXene layers. Based on the experimental results, the following mechanism has been suggested for the generation of 2D Ti_3C_2 MXene nanosheets:

$$Ti_3AlC_2 + 3HF = AlF_3 + 1.5H_2 + Ti_3C_2$$

$$Ti_3C_2 + 2H_2O = Ti_3C_2(OH)_2 + H_2$$

$$Ti_3C_2 + 2HF = Ti_3C_2F_2 + H_2$$

Various MXenes are produced by HF treatment under different synthesis conditions such as the concentration of HF, and etching time. However, due to the toxic nature of HF, other etching etchants such as ammonium bifluoride (NH_4HF_2) are also used. Other fluoride salts such as NaF, NH_4F, CaF_2, and FeF_3 mixtures with HCl have also been used as etchants in place of HF.[56,57] Similar to graphene, MXenes can also be synthesized by an electrochemical exfoliation method.

Due to higher electrical conductivity and large surface area, MXene/graphene composites are also developed for many potential applications. MXenes/graphene composites can be synthesized using both physical and chemical methods. A nanocomposite film was prepared by using a mixed solution of $Ti_3C_2T_x$/rGO.[58] Furthermore, Gogotsi *et al.* prepared a flexible MXene/rGO composite film for ultrafast supercapacitor applications by a self-assembly method.[59] The film was obtained *via* electrostatic self-assembly due to the positive charge of rGO sheets and the negative charge of MXene nanosheets. The as-obtained composite films showed that the interspersed MXene sheets increase the interlayer spacing between graphene sheets, which causes rapid diffusion and transport of electrolyte ions. Zhao *et al.* prepared a porous composite structure *via* a hydrothermal reaction of electrostatically self-assembled $Ti_3C_2T_x$/rGO, as shown in Fig. 4.[60] Known amounts of GO and $Ti_3C_2T_x$ were first mixed and a self-assembled structure was formed *via* electrostatic interactions. The as-obtained hydrogel was directionally frozen using an ice template, followed by hydrothermal treatment.

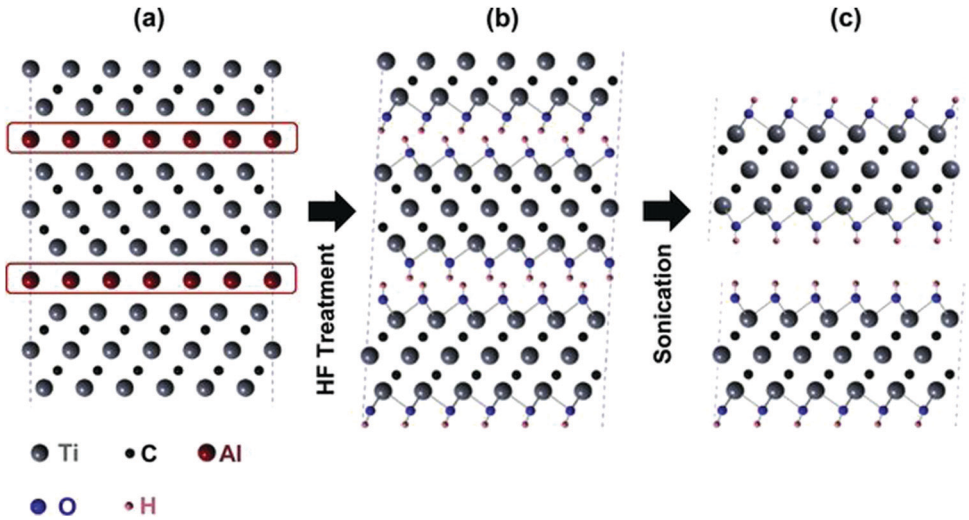

Fig. 3 Schematic of exfoliation process for Ti_3C_2 Mxene layers: (a) Max phase, (b) HF treatment, and (c) sonication process for the preparation of MXene. Reproduced with permission from ref. 55.

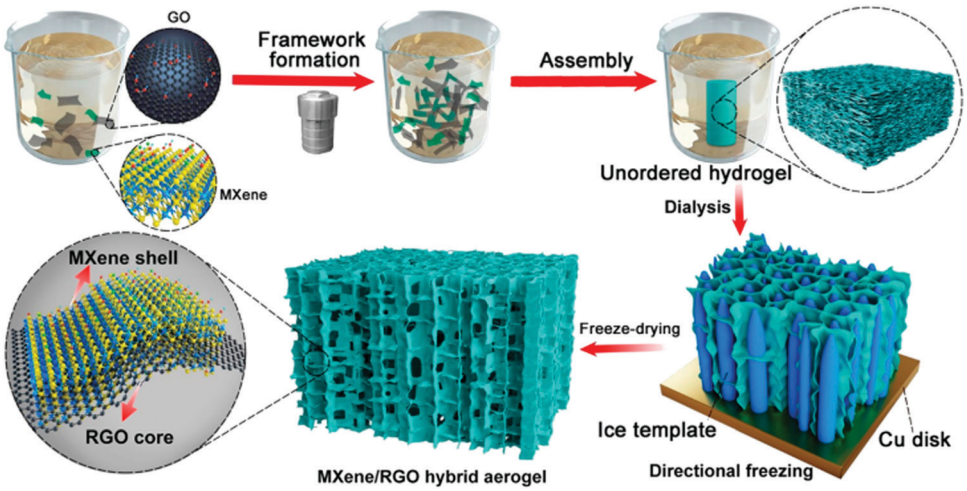

Fig. 4 Proposed mechanism of the $Ti_3C_2T_x$/rGO hybrid aerogel. Reproduced with permission from ref. 60.

The synthesis of MXene/graphene composites has also been reviewed elsewhere.[31]

3. Antimicrobial behaviour of MXenes and MXene–graphene composites

From ages, microbial infections and infectious diseases are the leading cause of death globally.[61] To avert the infection chances in serious health conditions including deep burn injuries and diabetic ulcers and in case of existent infection instances, the multiple-dose administration of the antibiotics is the most adopted therapeutic option. In addition, the overdosage of these antibiotics is accountable for creating multiple-drug resistant pathogens and superbugs, which are the biggest threat to human health worldwide.[62] These antibiotic-resistant pathogens cannot be inhibited by most of the existent antibiotics, and they are responsible for ~1 million deaths every year. As estimated, this number would be increased to 10 million by 2050, if appropriate actions are not taken.[62,63] This urges healthcare researchers to discover new antibacterial agents to alleviate the gradual resistance phenomenon of various microbial pathogens. In the last decade, a number of 2D materials including graphene oxide, MoS_2, and MXenes were explored for their antimicrobial activities, and their possible mechanisms of action were discovered. These materials have revealed excellent bactericidal properties against both Gram-positive and Gram-negative bacteria *via* rupturing the cell membrane, enhanced permeability across the membrane, DNA destruction, reduced metabolic activity and stress induced on the cell membrane by the sharp edges of the 2D materials as key modes of antimicrobial action.[64–66] Best owed with high surface area, richness in the chemical functionalities that provides feasibility of chemical alterations and functionalization, and enriched with nucleophilic moieties such as OH, F, or O that can mediate the attachment of antimicrobial metallic adjuvants *via* coordination chemistry, MXenes are rising as promising candidates to inhibit the bacterial and fungal growth.

Rasool *et al.* evaluated and compared the antibacterial activity of MAX phase (Ti_3AlC_2), single-layered exfoliated (S-$Ti_3C_2T_x$) and few-layered unexfoliated (F-$Ti_3C_2T_x$) MXene sheets against Gram-positive *B. subtilis* and Gram-negative *E. coli* bacteria.[65] The order of the antimicrobial activity against both the bacterial strains was reported as S-$Ti_3C_2T_x$ ≫ F-$Ti_3C_2T_x$ > Ti_3AlC_2, indicating the important role of the MXene thickness in determining their antimicrobial effects. Furthermore, the bacterial viability studies and optical density (OD) growth curves showed dose-dependent bactericidal properties of MXenes for both the investigated strains. They also compared the antimicrobial activity of $Ti_3C_2T_x$ with GO (well-noted 2D material for its antimicrobial properties) and demonstrated greater antibacterial activity of MXenes against *B. subtilis* and *E. coli* bacteria than GO. This shows the huge potential of novel 2D materials, namely, MXenes for antimicrobial applications. They have also studied the mechanism of antibacterial action for MXenes employing lactate dehydrogenase (LDH) release assay and different microscopic techniques including SEM and TEM and unveiled that bacterial toxicity posed by studied MXenes is attributed to cell membrane disruption and reactive oxygen species (ROS) production. In another study, Rasool *et al.* have reported the fabrication of a micrometer-thick $Ti_3C_2T_x$ MXene-based antibacterial membrane that can prevent bacterial adhesion and biofilm formation on the surface of separation membranes, which are responsible for their blocking.[67] Freshly prepared MXene-based membranes exhibited an antibacterial rate of 67% and 73% against *E. coli* and *B. subtilis* compared to the PVDF membrane as control. Interestingly, the aged or oxidized MXene membrane has shown more than 99% antibacterial efficiency. The designed membrane, with good bactericidal features against common waterborne bacteria, was reported to be useful as an anti-biofouling membrane for desalination of sea water. Differing from these studies that reveal outstanding bactericidal properties of $Ti_3C_2T_x$ MXene, Jastrzebska *et al.* reported a lack of antibacterial activity of

Ti_2CT_x MXenes against *Sarcina*, *S. aureus* and *Bacillus* sp.[68] In fact, the proliferation of the bacterial cells was found to be slightly intensified in the vicinity of Ti_2CT_x MXenes and only minor apoptosis of bacterial cells was observed when the cells were positioned between individual sheets of exfoliated Ti_2C. Comparison among the results reported by Rasool *et al.* and Jastrzębska *et al.* specifies that the stoichiometry of the MXene plays a pivotal role in deciding its bactericidal properties. To further validate these inferences, Jastrzębska *et al.* have compared the antibacterial efficiency of Ti_2C and Ti_3C_2 MXene phases, synthesized under the same operational conditions from their parent MAX phases.[69] The investigations showed that the Ti_3C_2 MXene phase has antimicrobial effectiveness against *E. coli*, whereas, Ti_2C did not show any bactericidal properties. The results of this study indicate that the structure at the atomic scale may play a key role in the bioactivity of MXenes of the same chemical composition, but with different stoichiometry techniques.

In the aforementioned reports, the MXenes have shown to exhibit antimicrobial effectiveness for limited bacterial strains that include *E. coli* and *B. subtilis*. To broaden the antimicrobial window of MXenes, Wu *et al.* proposed the integration of MXenes and near-infrared light (808 nm) and showed the effectiveness of this strategy against 15 different microbial strains including antibiotic-resistant strains namely methicillin-resistant *Staphylococcus aureus* (MRSA) and vancomycin-resistant *Enterococci* (VRE).[70] Interestingly, this photothermal ablation-based antimicrobial approach was also found to be very effective in eradicating MRSA biofilms. The killing of the bacteria *via* physical contact and photothermal effect is reported to be the main mode of antimicrobial action in this study. Shamsabadi *et al.* have recently investigated the antimicrobial mechanism of action of $Ti_3C_2T_x$ MXene nanosheets by exposing the bacterial samples (*E. coli* and *B. subtilis*) with 100 μg mL^{-1} colloidal solutions of MXene sheets of varying average lateral sizes (0.09, 0.35, 0.57 and 4.40 μm) using broth microdilution assay, fluorescence imaging (FI) and flow cytometry (FC) protocols.[66] This study indicated that the direct physical interaction between the bacterial membrane and the sharp edges of the MXene nanosheets plays a crucial role in determining their antimicrobial efficacy (Fig. 5). Based on the outcomes, the authors proposed that the $Ti_3C_2T_x$ MXene nanosheets with sharp edges get into the bacterial cytoplasmic region by cutting through the cell wall of the bacteria, resulting in DNA leakage and eventually bacterial cell disruption. Furthermore, the FC and FI results indicated that the antimicrobial activity of the MXene nanosheets is size and exposure time-dependent. The MXene sheets with smaller sizes are found to be more destructive towards the bacterial cells, particularly, if exposed for a longer duration. Treating the bacterial inoculum with 0.09–4.40 μm $Ti_3C_2T_x$ MXene nanosheets for 8 h in the darkness leads to >90% bacterial killing, whereas, 95% DNA content was found to be released from the bacterial cytosol.

Antimicrobial synergism between MXenes and metal nanostructures was also explored in some of the recent studies to design more efficient MXene-based antibacterial formulations.

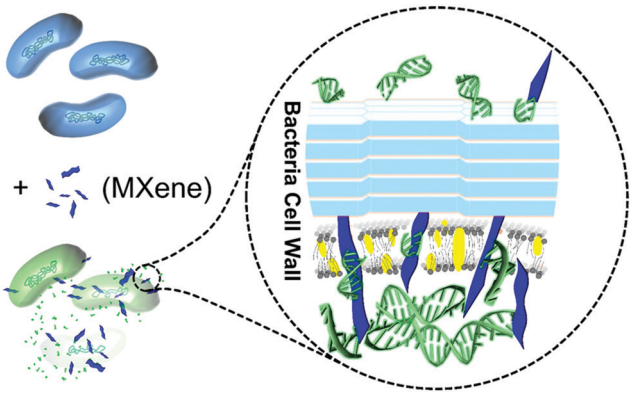

Fig. 5 Proposed antibacterial mechanism of action for MXene nanosheets. Reproduced with permission from ref. 66.

In this context, Pandey *et al.* reported an Ag nanoparticle (NP)-incorporated $Ti_3C_2T_x$ MXene-based antifouling composite membrane for water purification applications.[71] The AgNPs@$Ti_3C_2T_x$ MXene-based composite membranes were designed with different percentages of AgNP loading. The detailed structural and morphological characterizations confirm the presence of AgNPs within the MXene layers, which create the slit interspacing of 1–4 nm. These nano-dimensional spaces act as channels to flow the water and lead to the manufacturing of high-water flux membranes. Compared to the pristine PVDF membrane, 99% bacterial inhibition was recorded for AgNPs@$Ti_3C_2T_x$ MXene-based membranes and 60% for $Ti_3C_2T_x$ MXene-membranes. The enhanced antimicrobial activity in AgNP-decorated membranes may be due to the synergism in the antimicrobial capabilities of AgNPs and MXenes as well as owing to strong electrostatic interactions among negatively charged bacterial cell membranes and positively charged AgNPs@$Ti_3C_2T_x$ MXene surfaces. The SEM studies again confirmed the membrane targeting antimicrobial mechanism for AgNPs@$Ti_3C_2T_x$ MXenes. Lately, Zheng *et al.* reported the development of a novel antimicrobial agent through the conjugation of ultra-small gold nanoclusters (AuNCs, size <2 nm) on the $Ti_3C_2T_x$ MXene surface to achieve synergistic antimicrobial competence.[72] Regarding the mechanism of antimicrobial synergism, the MXene nanosheets first physically damage the bacterial cell due to their sharp edges that help in better internalization of AuNCs that generate ROS for bacterial membrane and DNA oxidation that eventually lead to bacterial cell death for both Gram-positive and Gram-negative bacteria. In the same study, authors reported the construction of crumpled MXene–AuNC structures to inhibit bacterial biofilm formation. The biofilm inhibition was reported to be due to the synergistic antimicrobial properties of MXene–AuNC conjugation, hydrophobicity of crumpled structures that prevent bacterial adhesion and high surface area of crumbled structures that carry high density bactericidal moieties for enhanced antimicrobial efficacy. For wound care applications, Mayerberger *et al.* developed nanofibrous antimicrobial wound dressing materials by encapsulating delaminated $Ti_3C_2T_x$ (MXene) flakes within chitosan nanofibers.[73] The 0.75% $Ti_3C_2T_x$-loaded dressings were tested against *E. coli* and *S. aureus* strains and the results revealed 95% and 62%

reduction, respectively, in the bacterial colony-forming units after 4 h of incubation. The nanofibrous mats were further found to be biocompatible in nature.

4. Photo-thermal and photocatalytically driven sterilization

MXenes exhibit excellent optical and electromagnetic properties, and they have considerably gained scientific and technological interests. Jhon *et al.* demonstrated the application of MXenes as saturable absorbers.[74] Jhon *et al.* also employed Ti_3C_2 MXenes to develop a terahertz detector.[75] Choi *et al.* demonstrated the use of Ti_3C_2 MXenes with metamaterials for terahertz shielding.[76] Li *et al.*[77] demonstrated the conversion of light into heat by employing titanium carbide MXenes. Huang *et al.*[78] suggested that the MXenes, in particular Ti_3C_2, can be exploited to achieve almost 100% photon-to-heat conversion. Thus, outstanding response of MXenes to light could also be harnessed to develop efficient healthcare and hygiene systems. Furthermore, MXenes also show hydrophilic behavior, which is important not only for many engineering and nanotechnological applications but also for biomedical applications.[24] The combined hydrophilic and light-to-heat conversion characteristics of MXenes can kill the microbes by dual actions, namely, (i) the microorganisms would make intimate contacts with sharp edges of the MXene that would rupture their cell membranes, and (ii) the generated heat would efficiently transfer to the microorganisms that intimately contacted, which effectively deactivates the microorganisms. Due to this principle, the MXene-based materials could be employed for the development of high-performance photo-sterilizers. Graphene and its derivatives also show excellent photon absorbing characteristics[79,80] and hence good light-to-heat conversion property. This photon-to-heat conversion property of graphene and its derivatives enables their application in phototherapy.[81] Addition of graphene or its derivatives to MXenes can further boost the photo-thermal properties of the resulting composites, which could lead to enhanced healthcare applications of MXene–graphene composites. Recently, Li *et al.*[82] have developed Bi_2S_3/$Ti_3C_2T_x$ MXene Schottky junctions and carried out interface engineering based on work function. The engineering of work function helps to enhance the charge transfer and hence photocatalytic activity, which resulted in fast killing of the bacteria.

Next, photoresponse and electrical conductivity of MXenes can greatly be engineered *via* surface functionalization.[83,84] Carbide MXenes with functional groups, in particular, show semiconducting behavior, which enables their potential photocatalytic properties. The carbide MXenes with functional groups such as Ti_2CO_2, Zr_2CO_2, and Hf_2CO_2 have shown excellent photocatalytic properties.[83,84] Furthermore, carbide MXene Ti_3C_2 has been either explored as a co-catalyst on metal sulfide absorbers[85] or employed as a reinforcing agent in TiO_2/Ti_3C_2 composites[86] for photocatalytic applications. The photocatalytic properties of MXenes can enable their application for deactivating viruses or bacteria. Graphene-based materials have also shown appealing photocatalytic properties.[87] Thus, composites of MXene–graphene composites are also promising options for developing smart photocatalytic principle-driven sterilizers for combating current and future pandemics.

5. MXene-based foams for healthcare applications

Foams are porous, light-weight, and low-density materials, which could be made up of a wide variety of materials, such as metals, ceramics, and polymers, and find widespread electronic, mechanical, energy, separation and engineering applications. In the recent past, MXene-based foams have attracted huge attention due to their exceptional functional properties. Liu *et al.*[88] developed MXene foams from the MAX phase by a three-step process: (i) first, Ti_3C_2 Mxene sheets were prepared by selective etching of Ti_3AlC_2, (ii) second, Mxene sheets were converted into a film by a vacuum-based filtration process, and (iii) third, the hydrazine treatment of Mxene films resulted in the formation of MXene foams (Fig. 6a). The developed MXene foam showed excellent electromagnetic interference shielding performance. Lin *et al.*[89] prepared MXene–GO hybrid foams by a gelation process for application in terahertz radiation shielding (Fig. 6c). Wu *et al.*[90] proposed a two-step process involving the development of 3D MXene aerogels followed by its conversion into the foam with PDMS coating for structural stability. Ma *et al.*[91] developed an MXene/GO hybrid foam by a solvothermal method with tunable high-performance stealth characteristics (Fig. 6b). Zhao *et al.*[92] prepared a macroporous 3D MXene network, namely, MXene foam by applying MXene sheets on melamine foam structures. Yin *et al.* synthesized an MXene foam with silver nanowires for enhanced electromagnetic interference shielding applications.[93] Jia *et al.* developed conductive polymer/Mxene composite foams, and by employing only 0.0225 vol% of MXenes in composite foams, a significant electromagnetic shielding was realized.[94]

Since MXenes hold promising antimicrobial properties, the foam structures of MXenes have tremendous potential for healthcare applications. For example, the MXene foams can be employed for filtration purposes in healthcare systems. One such demanding component in pandemic time is high-quality face mask. Since the vaccine and medicine developments take enormous time, face mask should be considered as a substitute of vaccines/medicines until the latter has developed. Currently, N95 face mask (a standard of the United States) is commonly used by healthcare workers. Similarly, KN95, FFP2, P2, DS2, and Korea 1st class are the Chinese, European, Australian/New Zealand, Japan and South Korean standards of N95 equivalent face masks, respectively. These face masks always work on the barrier principle, *i.e.* they stop the contaminant particles to transmit through it and protect humans from catching up with the infection. However, such particles always present/adhere onto the surface of the mask/filter. The survival time of such adhered contaminant particles (viruses or bacteria) could be from few hours to few days. This poses a major risk to human health. MXene foams with tunable porosities and pore sizes

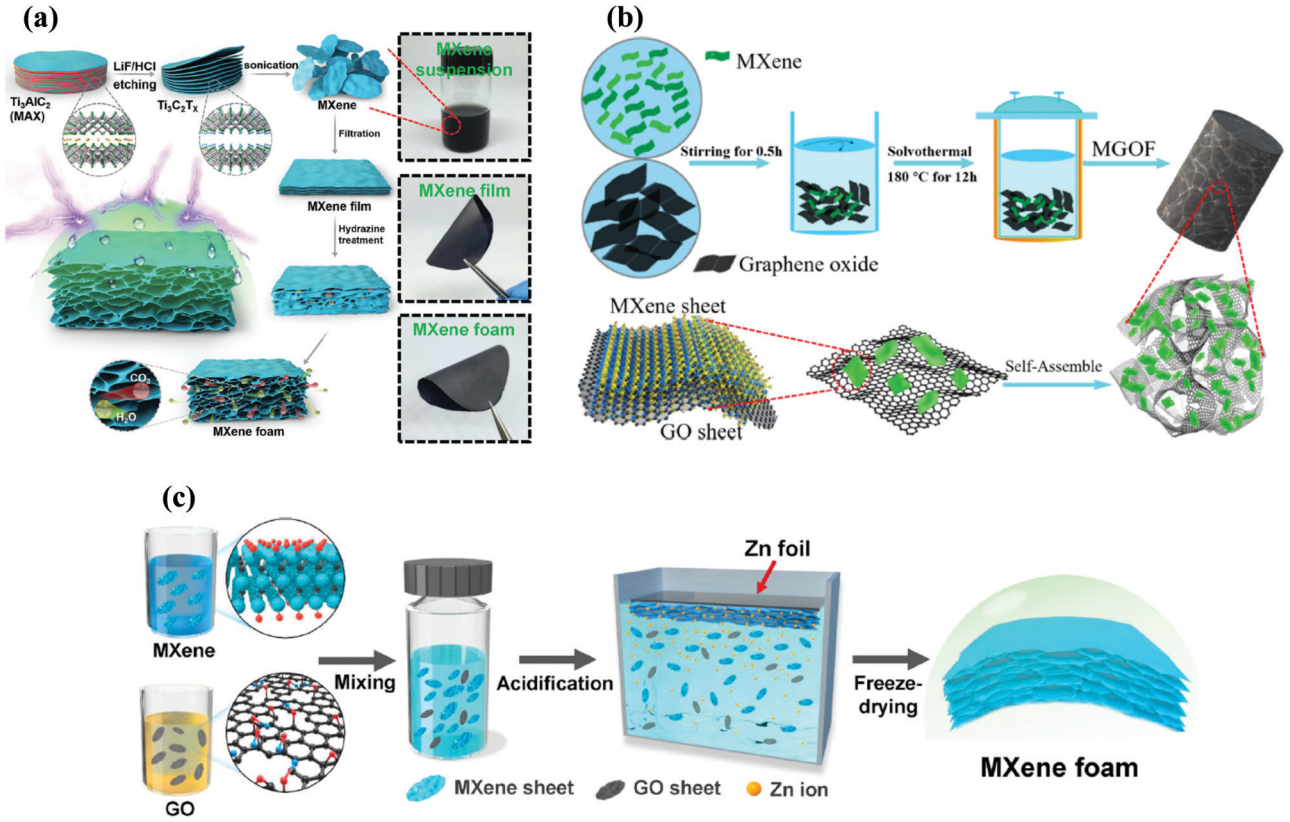

Fig. 6 Development of MXene foams: (a) MXene film-to-foam conversion (reproduced with permission from ref. 88), (b) synthesis of MXene–GO hybrid foams by self-assembly of GO and MXene sheets (reproduced with permission from ref. 91), and (c) synthesis of MXene–GO foams by a gelation process (reproduced with permission from ref. 89).

could be developed and explored for the development of advanced face masks. Importantly, such materials would not just stop the contaminant particles but also kill the adhered microorganisms due to the inherent antimicrobial activity of MXenes. Since graphene and its derivatives also show excellent antibacterial and antiviral properties and offer feasibility to engineer their pore size, MXene–graphene composite-based foams are also promising options for the development of high-performance face masks.

6. MXene and MXene–graphene composites for PPE development

Most of the PPEs such as jump suits, aprons, and face masks are made up of polypropylene (PPy). However, what is critical here is that after their single use, these items need to be disposed. This brings another major problem of plastic waste and raises a critical environmental concern. Additionally, due to single use, the replacement cost of PPEs is also very high as the wearers change the PPEs several times in a day. MXenes, graphene and their derivatives can be applied on cloths, plastics including PPy, glass, *etc.*[95] Thus, due to their inherent antimicrobial properties, graphene, MXene and MXene–graphene composite-coated PPEs are promising alternatives for the development of reusable PPEs and can solve major plastic waste problems. Bhattacharjee *et al.* comprehensively discussed the graphene-modified polymers and textiles for the development of smart PPEs.[96] Similarly, MXenes and 1–2 layers of graphene are considerably transparent. Thus, the MXene or MXene–graphene composite-based antimicrobial coatings can also be applied on face shields, medical spectacles, *etc.*, for their long-term use. Furthermore, various architectures of MXenes and their composites can be developed using advanced manufacturing tools such as 3D printing for various applications.[97–99] This also opens up the possibility for utilization of additive manufacturing for the development of healthcare components such as respirators, face shields, and components of ventilators.

7. MXenes and its composites for biosensor development

MXenes are attracting remarkable attention towards the development of optical and electrochemical biosensor devices[100,101] owing to their (i) excellent physical, chemical, optical and electrochemical properties; (ii) –OH, C═O and –F groups enriched chemical structures that will provide active sites for biomolecule immobilization; (iii) accordion-like multilayered architecture that provides high surface area for enzyme loading and electrocatalytic processes; (iv) antifouling and anti-passivation features; and (v) good biocompatibility substantiated by the

retained long-term enzyme activity over the MXene surface.[102] Yoon *et al.* summarized the literature on MXene-nanocomposite-based electrochemical and optical biosensors.[103] Peng *et al.* have demonstrated MXene nanosheet (Ti_3C_2 NS)-based fluorescence DNA biosensors for the selective detection of human papilloma virus (HPV, a causative agent for cervical cancer) using high fluorescence quenching ability of MXenes for fluorescence dyes and their varied affinities for ssDNA *versus* dsDNA (Fig. 7a).[100] Under the fluorescence quenching effect of Ti_3C_2 NS, a ssDNA probe (P) shows slight fluorescence emission. After the duplex formation following hybridization with its complementary target, ssDNA (T), the fluorescence intensity enhances evidently. Exonuclease III (Exo III) was employed to improve the sensitivity by promoting more fluorescence enhancement. This magnified fluorescent sensor for HPV-18 detection shows a low detection limit of 100 pM with high specificity. Furthermore, the developed DNA sensor can be used to determine PCR-amplified HPV-18 from cervical scrape samples. It highlights ultrathin Ti_3C_2 NS as a potential candidate for the construction of fluorescence DNA biosensors with excellent performances. Similar strategies can be adopted for the detection of COVID-19 using MXenes as a transducer platform targeting virus RNA, virus surface antigens/antibodies, whole virions, or other potential biomarkers. For example, ssDNA probe (with/without the fluorescent dye) specific to virus RNA can be immobilized on the MXene surface and employed for optical and electrochemical sensing of virus RNA; the MXene surface can be functionalized with SARS-CoV-2 spike S1 subunit protein antibody (CS1Ab) or ACE2 receptors (Fig. 7b). This arrangement can be used to detect COVID-19 electrochemically or by designing field-effect transistor-based biosensing systems; MXenes can be modified with the spike protein S1 antigen and can be used to screen the coronavirus-neutralizing antibodies.

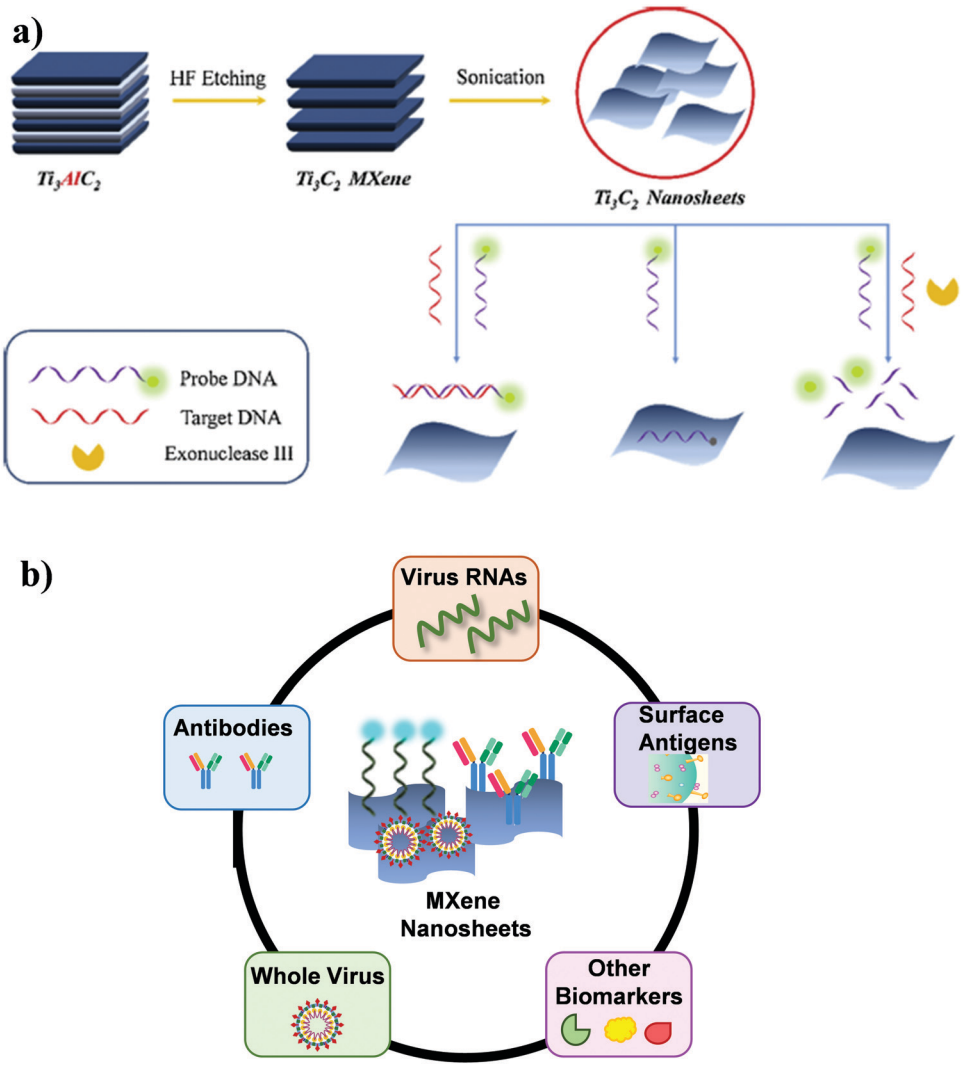

Fig. 7 (a) Illustration of the analysis of HPV-18-specific DNA target using MXene nanosheet-based off–on fluorescent nanoprobes, reproduced with permission from ref. 100. (b) Pictorial representation of various approaches towards the development of the MXene nanosheet-based biosensors for SARS-CoV-2 detection targeting virus RNA, surface antigen, whole virus, antibodies and other biomarkers in human samples.

8. Biocompatibility and cytotoxicity assessment of MXenes

In the recent past, MXenes and other 2D materials have drawn enormous attention for different biomedical applications. However, to validate the utility of a material for biomedical applications, its cytotoxicity evaluation is also one of the key requirements. Regarding the cytotoxicity of the MXenes, an ecotoxicological study was reported employing a zebrafish embryo model to reveal indirectly the impact of these novel MXene-based materials on the human biological system.[104] The neurotoxicity and locomotion assessment of this *in vivo* study displays a similar number of neurons in the spinal cord part of the $Ti_3C_2T_x$-incubated zebrafish embryos and dimethyl sulfoxide negative control, indicating no adverse toxicological impact of MXenes on the muscle activity and neurons of the zebrafish. Primarily, as the lethal concentration 50 (LC50) of $Ti_3C_2T_x$ was found to be more than 100 μg mL^{-1}, the $Ti_3C_2T_x$ MXene could be classified under the ''practically nontoxic'' group as per Acute Toxicity Rating Scale by the Fish and Wildlife Service (FWS). In another *in vivo* mouse study, the hemocompatibility and excretion evaluation of Ti_3C_2-SP nanosheets have been performed.[105] Different doses of Ti_3C_2-SP nanosheets were intravenously administered into the mouse body, and the histomorphology and pathological changes in the major organs after the treatment have been assessed.[105] The results indicate no obvious acute toxicity and side effects with high histocompatibility. Importantly, Ti_3C_2-SP nanosheets were found to be gradually excreted out of the body *via* feces and urine with total excretory amounts of 10.35% and 10.35%, respectively.[105] In another systematic 30 days *in vivo* biocompatibility study using MnO_x/Ti_3C_2-SP composite nanosheets, insignificant toxicity was reported after its intravenous administration into healthy mice at different dose levels.[106] The preliminary results in the form of no significant body loss, no substantial variation in blood, liver and kidney cell indexes and no obvious tissue damage during the whole feeding period indicate their low biotoxicity and good biocompatibility, which further guarantee their potential clinical translational applications.[106] Furthermore, the *in vivo* biocompatibility of surface-modified MXene nanosheets against mice was comprehensively evaluated.[107] The healthy Kunming mice were divided into three treated groups (exposed with NIR-I, NIR-II and daylight) and one control group incubated with three dosages of surface-modified MXenes (Ta_4C_3-SP dosage of 20 mg kg^{-1}) at day 1, 7 and 28.[107] Negligible abnormalities in terms of behaviour, body weight, biochemical parameters, and hematological indexes were observed in the treatment groups compared with the control group, confirming no chronic pathological toxicity related to the investigated MXene composite.[107] Similar evaluation was also performed on Ti_3C_2 and Ta_4C_3 MXenes, which also highlights their good biocompatibility and negligible cytotoxicity.[108,109] Although, the reported *in vitro* and *in vivo* studies corroborated the benignness and biosafety of MXenes and MXene composites and also authorize their appropriateness towards different biomedical applications, however, detailed genotoxicity and reproductivity toxicity are essentially required to confirm their clinical and translational potentials.

9. Conclusions and future prospects

MXenes have shown great promise for biomedical applications. In this review, we compiled the studies and discussed antimicrobial, photocatalytic and photothermal, electrical, surface functionalization, wettability properties, *etc.*, of MXenes. The high electrical conductivity combined with surface functionalization feasibility would facilitate the binding of biomolecules on their surface, and make MXenes the ideal candidates for the development of fast and sensitive diagnosis devices, for example, biosensors, which could be utilized for the early detection of viral infections. Antimicrobial properties can lead to their applications in the development of reusable face masks and shields, medical aprons, spectacles, *etc.* Photocatalytic and photothermal properties of MXenes make them the potential candidates for high-performance photo sterilizers. MXenes can be developed in foam forms, which are required for the development of some PPEs. MXene-based components can be made by advanced manufacturing processes like 3D printing, which can also be utilized for the development of PPEs and components for medical equipment. Graphene and its derivatives also display many such fascinating properties. Therefore, MXene–graphene composites are also potential candidates for the development of improved diagnostic devices, PPEs, and many other medical systems/components, which are essentially required in pandemic time.

Although MXenes were discovered about ten years ago, their antimicrobial properties have been discovered very recently about three years back. Additionally, there are only a few reports pertaining to the development of MXene-based biosensors for the detection of pathogens. Furthermore, although excellent photocatalytic and photothermal properties have been found in MXenes, their direct uses in the development of medical components remain few and far between. Similarly, the direct use of MXenes for the development of PPEs is not reported to date despite their antimicrobial properties, but they can be coated on a wide variety of surfaces and can be made in foam forms. Thus, though the MXenes are promising materials for biomedical applications, the path for their commercial biomedical products is quite long. However, this article would certainly open the door to explore MXenes and MXene–graphene composites for the designing and development of biomedical components, especially those required for combating pandemics.

Conflicts of interest

There are no conflicts to declare.

References

1 https://www.history.com/topics/middle-ages/pandemics-timeline.
2 Y. Yang, A. M. Asiri, Z. Tang, D. Du and Y. Lin, Graphene based materials for biomedical applications, *Mater. Today*, 2013, **16**, 365–373.

3 C. Chung, Y.-K. Kim, D. Shin, S.-R. Ryoo, B. H. Hong and D.-H. Min, Biomedical applications of graphene and graphene oxide, *Acc. Chem. Res.*, 2013, **46**, 2211–2224.
4 A. Srivastava, N. Dwivedi, C. Dhand, R. Khan, N. Sathish, M. K. Gupta, R. Kumar and S. Kumar, Potential of Graphene-based Materials to Combat COVID-19: Properties, Perspectives and Prospects, *Mater. Today Chem.*, 2020, 100385.
5 A. Geim and K. Novoselov, The rise of graphene, *Nat. Mater.*, 2007, **6**, 183–191.
6 A. C. Ferrari, F. Bonaccorso, V. Fal'Ko, K. S. Novoselov, S. Roche, P. Bøggild, S. Borini, F. H. Koppens, V. Palermo and N. Pugno, Science and technology roadmap for graphene, related two-dimensional crystals, and hybrid systems, *Nanoscale*, 2015, **7**, 4598–4810.
7 R. Pasricha, S. Gupta and A. K. Srivastava, A facile and novel synthesis of Ag–graphene-based nanocomposites, *Small*, 2009, **5**, 2253–2259.
8 N. O. Weiss, H. Zhou, L. Liao, Y. Liu, S. Jiang, Y. Huang and X. Duan, Graphene: an emerging electronic material, *Adv. Mater.*, 2012, **24**, 5782–5825.
9 N. Dwivedi, T. Patra, J.-B. Lee, R. J. Yeo, S. Srinivasan, T. Dutta, K. Sasikumar, C. Dhand, S. Tripathy and M. S. Saifullah, Slippery and Wear-Resistant Surfaces Enabled by Interface Engineered Graphene, *Nano Lett.*, 2019, **20**, 905–917.
10 M. D. Mukherjee, C. Dhand, N. Dwivedi, B. P. Singh, G. Sumana, V. V. Agarwal, J. S. Tawale and B. D. Malhotra, Facile synthesis of 2-dimensional transparent graphene flakes for nucleic acid detection, *Sens. Actuators, B*, 2015, **210**, 281–289.
11 J. K. Tiwari, A. Mandal, N. Sathish, A. Agrawal and A. Srivastava, Investigation of porosity, microstructure and mechanical properties of additively manufactured graphene reinforced AlSi10Mg composite, *Additive Manufacturing*, 2020, **33**, 101095.
12 H. E. Karahan, C. Wiraja, C. Xu, J. Wei, Y. Wang, L. Wang, F. Liu and Y. Chen, Graphene materials in antimicrobial nanomedicine: current status and future perspectives, *Adv. Healthcare Mater.*, 2018, **7**, 1701406.
13 X. Zou, L. Zhang, Z. Wang and Y. Luo, Mechanisms of the antimicrobial activities of graphene materials, *J. Am. Chem. Soc.*, 2016, **138**, 2064–2077.
14 N. Dwivedi, N. Satyanarayana, R. J. Yeo, H. Xu, K. P. Loh, S. Tripathy and C. S. Bhatia, Ultrathin carbon with interspersed graphene/fullerene-like nanostructures: a durable protective overcoat for high density magnetic storage, *Sci. Rep.*, 2015, **5**, 1–16.
15 F. Shahzad, P. Kumar, S. Yu, S. Lee, Y.-H. Kim, S. M. Hong and C. M. Koo, Sulfur-doped graphene laminates for EMI shielding applications, *J. Mater. Chem. C*, 2015, **3**, 9802–9810.
16 P. Kumar, F. Shahzad, S. M. Hong and C. M. Koo, A flexible sandwich graphene/silver nanowires/graphene thin film for high-performance electromagnetic interference shielding, *RSC Adv.*, 2016, **6**, 101283.
17 F. Koppens, T. Mueller, P. Avouris, A. Ferrari, M. Vitiello and M. Polini, Photodetectors based on graphene, other two-dimensional materials and hybrid systems, *Nat. Nanotechnol.*, 2014, **9**, 780–793.
18 G. Seo, G. Lee, M. J. Kim, S.-H. Baek, M. Choi, K. B. Ku, C.-S. Lee, S. Jun, D. Park and H. G. Kim, Rapid detection of COVID-19 causative virus (SARS-CoV-2) in human nasopharyngeal swab specimens using field-effect transistor-based biosensor, *ACS Nano*, 2020, **14**, 5135–5142.
19 V. Palmieri and M. Papi, Can graphene take part in the fight against COVID-19?, *Nano Today*, 2020, 100883.
20 A. Cordaro, G. Neri, M. T. Sciortino, A. Scala and A. Piperno, Graphene-Based Strategies in Liquid Biopsy and in Viral Diseases Diagnosis, *Nanomaterials*, 2020, **10**, 1014.
21 R. M. Torrente-Rodríguez, H. Lukas, J. Tu, J. Min, Y. Yang, C. Xu, H. B. Rossiter and W. Gao, SARS-CoV-2 RapidPlex: A Graphene-based Multiplexed Telemedicine Platform for Rapid and Low-Cost COVID-19 Diagnosis and Monitoring, *Matter*, 2020, **3**, 1981–1998.
22 Y. Gogotsi and B. Anasori, The rise of MXenes, *ACS Nano*, 2019, **13**, 8491–8494.
23 H. Lin, Y. Chen and J. Shi, Insights into 2D MXenes for versatile biomedical applications: current advances and challenges ahead, *Adv. Sci.*, 2018, **5**, 1800518.
24 C. Weiss, M. Carriere, L. Fusco, I. Capua, J. A. Regla-Nava, M. Pasquali, J. A. Scott, F. Vitale, M. A. Unal and C. Mattevi, Toward Nanotechnology-Enabled Approaches against the COVID-19 Pandemic, *ACS Nano*, 2020, **14**, 6383–6406.
25 W. Eom, H. Shin, R. B. Ambade, S. H. Lee, K. H. Lee, D. J. Kang and T. H. Han, Large-scale wet-spinning of highly electroconductive MXene fibers, *Nat. Commun.*, 2020, **11**, 1–7.
26 Y. Yang, Z. Cao, P. He, L. Shi, G. Ding, R. Wang and J. Sun, $Ti_3C_2T_x$ MXene–graphene composite films for wearable strain sensors featured with high sensitivity and large range of linear response, *Nano Energy*, 2019, **66**, 104134.
27 B. Aïssa, A. Ali, K. Mahmoud, T. Haddad and M. Nedil, Transport properties of a highly conductive 2D $Ti_3C_2T_x$ MXene/graphene composite, *Appl. Phys. Lett.*, 2016, **109**, 043109.
28 Y. Liu, K. Wu, M. Lu, E. Jiao, H. Zhang, J. Shi and M. Lu, Highly thermal conductivity and flame retardant flexible graphene/MXene paper based on an optimized interface and nacre laminated structure, *Composites, Part A*, 2021, **141**, 106227.
29 S. Zhao, H.-B. Zhang, J.-Q. Luo, Q.-W. Wang, B. Xu, S. Hong and Z.-Z. Yu, Highly electrically conductive three-dimensional Ti3C2T x MXene/reduced graphene oxide hybrid aerogels with excellent electromagnetic interference shielding performances, *ACS Nano*, 2018, **12**, 11193–11202.
30 V.-T. Nguyen, B. K. Min, Y. Yi, S. J. Kim and C.-G. Choi, MXene ($Ti_3C_2T_x$)/graphene/PDMS composites for multifunctional broadband electromagnetic interference shielding skins, *Chem. Eng. J.*, 2020, 124608.
31 Y. Liu, J. Yu, D. Guo, Z. Li and Y. Su, $Ti_3C_2T_x$ MXene/graphene nanocomposites: Synthesis and application in electrochemical energy storage, *J. Alloys Compd.*, 2020, **815**, 152403.
32 Y. Zhou, K. Maleski, B. Anasori, J. O. Thostenson, Y. Pang, Y. Feng, K. Zeng, C. B. Parker, S. Zauscher and Y. Gogotsi, $Ti_3C_2T_x$ MXene-Reduced Graphene Oxide Composite

Electrodes for Stretchable Supercapacitors, *ACS Nano*, 2020, **14**, 3576–3586.

33 X. Zhan, C. Si, J. Zhou and Z. Sun, MXene and MXene-based composites: synthesis, properties and environment-related applications, *Nanoscale Horiz.*, 2020, **5**, 235–258.

34 K. Tan, L. Samylingam, N. Aslfattahi, R. Saidur and K. Kadirgama, Optical and conductivity studies of polyvinyl alcohol-MXene (PVA-MXene) nanocomposite thin films for electronic applications, *Opt. Laser Technol.*, 2021, **136**, 106772.

35 W. Cao, C. Ma, S. Tan, M. Ma, P. Wan and F. Chen, Ultrathin and flexible CNTs/MXene/cellulose nanofibrils composite paper for electromagnetic interference shielding, *Nano-Micro Lett.*, 2019, **11**, 1–17.

36 L. P. Biró, P. Nemes-Incze and P. Lambin, Graphene: nanoscale processing and recent applications, *Nanoscale*, 2012, **4**, 1824–1839.

37 A. C. Ferrari, F. Bonaccorso, V. Fal'ko, K. S. Novoselov, S. Roche, P. Bøggild, S. Borini, F. H. L. Koppens, V. Palermo, N. Pugno, J. A. Garrido, R. Sordan, A. Bianco, L. Ballerini, M. Prato, E. Lidorikis, J. Kivioja, C. Marinelli, T. Ryhänen, A. Morpurgo, J. N. Coleman, V. Nicolosi, L. Colombo, A. Fert, M. Garcia-Hernandez, A. Bachtold, G. F. Schneider, F. Guinea, C. Dekker, M. Barbone, Z. Sun, C. Galiotis, A. N. Grigorenko, G. Konstantatos, A. Kis, M. Katsnelson, L. Vandersypen, A. Loiseau, V. Morandi, D. Neumaier, E. Treossi, V. Pellegrini, M. Polini, A. Tredicucci, G. M. Williams, B. Hee Hong, J.-H. Ahn, J. Min Kim, H. Zirath, B. J. van Wees, H. van der Zant, L. Occhipinti, A. Di Matteo, I. A. Kinloch, T. Seyller, E. Quesnel, X. Feng, K. Teo, N. Rupesinghe, P. Hakonen, S. R. T. Neil, Q. Tannock, T. Löfwander and J. Kinaret, Science and technology roadmap for graphene, related two-dimensional crystals, and hybrid systems, *Nanoscale*, 2015, **7**, 4598–4810.

38 K. Parvez, Z.-S. Wu, R. Li, X. Liu, R. Graf, X. Feng and K. Müllen, Exfoliation of Graphite into Graphene in Aqueous Solutions of Inorganic Salts, *J. Am. Chem. Soc.*, 2014, **136**, 6083–6091.

39 M. Alanyalıoğlu, J. J. Segura, J. Oró-Solè and N. Casañ-Pastor, The synthesis of graphene sheets with controlled thickness and order using surfactant-assisted electrochemical processes, *Carbon*, 2012, **50**, 142–152.

40 W. S. Hummers and R. E. Offeman, Preparation of Graphitic Oxide, *J. Am. Chem. Soc.*, 1958, **80**, 1339.

41 J. Chen, Y. Zhang, M. Zhang, B. Yao, Y. Li, L. Huang, C. Li and G. Shi, Water-enhanced oxidation of graphite to graphene oxide with controlled species of oxygenated groups, *Chem. Sci.*, 2016, **7**, 1874–1881.

42 P. Kumar, F. Shahzad, S. Yu, S. M. Hong, Y.-H. Kim and C. M. Koo, Large-area reduced graphene oxide thin film with excellent thermal conductivity and electromagnetic interference shielding effectiveness, *Carbon*, 2015, **94**, 494–500.

43 L. Peng, Z. Xu, Z. Liu, Y. Wei, H. Sun, Z. Li, X. Zhao and C. Gao, An iron-based green approach to 1-h production of single-layer graphene oxide, *Nat. Commun.*, 2015, **6**, 5716.

44 A. Ambrosi and M. Pumera, Precise Tuning of Surface Composition and Electron-Transfer Properties of Graphene Oxide Films through Electroreduction, *Chem. – Eur. J.*, 2013, **19**, 4748–4753.

45 G. Xin, H. Sun, T. Hu, H. R. Fard, X. Sun, N. Koratkar, T. Borca-Tasciuc and J. Lian, Large-Area Freestanding Graphene Paper for Superior Thermal Management, *Adv. Mater.*, 2014, **26**, 4521–4526.

46 U. Hofmann and E. König, Untersuchungen über Graphitoxyd, *Z. Anorg. Allg. Chem.*, 1937, **234**, 311–336.

47 S. Park, J. An, J. R. Potts, A. Velamakanni, S. Murali and R. S. Ruoff, Hydrazine-reduction of graphite- and graphene oxide, *Carbon*, 2011, **49**, 3019–3023.

48 H.-J. Shin, K. K. Kim, A. Benayad, S.-M. Yoon, H. K. Park, I.-S. Jung, M. H. Jin, H.-K. Jeong, J. M. Kim, J.-Y. Choi and Y. H. Lee, Efficient Reduction of Graphite Oxide by Sodium Borohydride and Its Effect on Electrical Conductance, *Adv. Funct. Mater.*, 2009, **19**, 1987–1992.

49 P. Kumar, S. Yu, F. Shahzad, S. M. Hong, Y.-H. Kim and C. M. Koo, Ultrahigh electrically and thermally conductive self-aligned graphene/polymer composites using large-area reduced graphene oxides, *Carbon*, 2016, **101**, 120–128.

50 W. Gao, L. B. Alemany, L. Ci and P. M. Ajayan, New insights into the structure and reduction of graphite oxide, Nature, *Chemistry*, 2009, **1**, 403–408.

51 P. Sutter, J. T. Sadowski and E. Sutter, Graphene on Pt(111): Growth and substrate interaction, *Phys. Rev. B: Condens. Matter Mater. Phys.*, 2009, **80**, 245411.

52 M. Losurdo, M. M. Giangregorio, P. Capezzuto and G. Bruno, Graphene CVD growth on copper and nickel: role of hydrogen in kinetics and structure, *Phys. Chem. Chem. Phys.*, 2011, **13**, 20836–20843.

53 X. Li, W. Cai, L. Colombo and R. S. Ruoff, Evolution of Graphene Growth on Ni and Cu by Carbon Isotope Labeling, *Nano Lett.*, 2009, **9**, 4268–4272.

54 X. Li, C. W. Magnuson, A. Venugopal, J. An, J. W. Suk, B. Han, M. Borysiak, W. Cai, A. Velamakanni, Y. Zhu, L. Fu, E. M. Vogel, E. Voelkl, L. Colombo and R. S. Ruoff, Graphene Films with Large Domain Size by a Two-Step Chemical Vapor Deposition Process, *Nano Lett.*, 2010, **10**, 4328–4334.

55 M. Naguib, M. Kurtoglu, V. Presser, J. Lu, J. Niu, M. Heon, L. Hultman, Y. Gogotsi and M. W. Barsoum, Two-Dimensional Nanocrystals Produced by Exfoliation of Ti_3AlC_2, *Adv. Mater.*, 2011, **23**, 4248–4253.

56 X. Wang, C. Garnero, G. Rochard, D. Magne, S. Morisset, S. Hurand, P. Chartier, J. Rousseau, T. Cabioc'h, C. Coutanceau, V. Mauchamp and S. Célérier, A new etching environment (FeF3/HCl) for the synthesis of two-dimensional titanium carbide MXenes: a route towards selective reactivity *vs.* water, *J. Mater. Chem. A*, 2017, **5**, 22012–22023.

57 V. M. Hong, Ng, H. Huang, K. Zhou, P. S. Lee, W. Que, J. Z. Xu and L. B. Kong, Recent progress in layered transition metal carbides and/or nitrides (MXenes) and their composites: synthesis and applications, *J. Mater. Chem. A*, 2017, **5**, 3039–3068.

58 H. Li, Y. Hou, F. Wang, M. R. Lohe, X. Zhuang, L. Niu and X. Feng, Flexible All-Solid-State Supercapacitors with High

Volumetric Capacitances Boosted by Solution Processable MXene and Electrochemically Exfoliated Graphene, *Adv. Energy Mater.*, 2017, **7**, 1601847.

59 J. Yan, C. E. Ren, K. Maleski, C. B. Hatter, B. Anasori, P. Urbankowski, A. Sarycheva and Y. Gogotsi, Flexible MXene/Graphene Films for Ultrafast Supercapacitors with Outstanding Volumetric Capacitance, *Adv. Funct. Mater.*, 2017, **27**, 1701264.

60 S. Zhao, H.-B. Zhang, J.-Q. Luo, Q.-W. Wang, B. Xu, S. Hong and Z.-Z. Yu, Highly Electrically Conductive Three-Dimensional $Ti_3C_2T_x$ MXene/Reduced Graphene Oxide Hybrid Aerogels with Excellent Electromagnetic Interference Shielding Performances, *ACS Nano*, 2018, **12**, 11193–11202.

61 https://www.who.int/whr/1996/media_centre/press_release/en/.

62 S. J. Howard, S. Hopwood and S. C. Davies, Antimicrobial resistance: a global challenge, in, American Association for the Advancement of Science, 2014.

63 R. Sugden, R. Kelly and S. Davies, Combatting antimicrobial resistance globally, *Nat. Microbiol.*, 2016, **1**, 1–2.

64 W. Sun and F. G. Wu, Two-Dimensional Materials for Antimicrobial Applications: Graphene Materials and Beyond, *Chem. – Asian J.*, 2018, **13**, 3378–3410.

65 K. Rasool, M. Helal, A. Ali, C. E. Ren, Y. Gogotsi and K. A. Mahmoud, Antibacterial activity of $Ti_3C_2T_x$ MXene, *ACS Nano*, 2016, **10**, 3674–3684.

66 A. Arabi Shamsabadi, M. Sharifian Gh, B. Anasori and M. Soroush, Antimicrobial Mode-of-Action of Colloidal $Ti_3C_2T_x$ MXene Nanosheets, *ACS Sustainable Chem. Eng.*, 2018, **6**, 16586–16596.

67 K. Rasool, K. A. Mahmoud, D. J. Johnson, M. Helal, G. R. Berdiyorov and Y. Gogotsi, Efficient antibacterial membrane based on two-dimensional $Ti_3C_2T_x$ (MXene) nanosheets, *Sci. Rep.*, 2017, **7**, 1–11.

68 A. Jastrzębska, E. Karwowska, D. Basiak, A. Zawada, W. Ziemkowska, T. Wojciechowski, D. Jakubowska and A. Olszyna, Biological activity and bio-sorption properties of the Ti2C studied by means of zeta potential and SEM, *Int. J. Electrochem. Sci.*, 2017, **12**, 2159–2172.

69 A. M. Jastrzębska, E. Karwowska, T. Wojciechowski, W. Ziemkowska, A. Rozmysłowska, L. Chlubny and A. Olszyna, The atomic structure of Ti_2C and Ti_3C_2 MXenes is responsible for their antibacterial activity toward E. coli bacteria, *J. Mater. Eng. Performance*, 2019, **28**, 1272–1277.

70 F. Wu, H. Zheng, W. Wang, Q. Wu, Q. Zhang, J. Guo, B. Pu, X. Shi, J. Li and X. Chen, Rapid eradication of antibiotic-resistant bacteria and biofilms by MXene and near-infrared light through photothermal ablation, *Sci. China Mater.*, 2020, 1–11.

71 R. P. Pandey, K. Rasool, V. E. Madhavan, B. Aïssa, Y. Gogotsi and K. A. Mahmoud, Ultrahigh-flux and fouling-resistant membranes based on layered silver/MXene ($Ti_3C_2T_x$) nanosheets, *J. Mater. Chem. A*, 2018, **6**, 3522–3533.

72 K. Zheng, S. Li, L. Jing, P. Y. Chen and J. Xie, Synergistic Antimicrobial Titanium Carbide (MXene) Conjugated with Gold Nanoclusters, *Adv. Healthcare Mater.*, 2020, **9**, 2001007.

73 E. A. Mayerberger, R. M. Street, R. M. McDaniel, M. W. Barsoum and C. L. Schauer, Antibacterial properties of electrospun $Ti_3C_2T_z$ (MXene)/chitosan nanofibers, *RSC Adv.*, 2018, **8**, 35386–35394.

74 Y. I. Jhon, J. Koo, B. Anasori, M. Seo, J. H. Lee, Y. Gogotsi and Y. M. Jhon, Metallic MXene saturable absorber for femtosecond mode-locked lasers, *Adv. Mater.*, 2017, **29**, 1702496.

75 Y. Jhon, M. Seo and Y. Jhon, First-principles study of a MXene terahertz detector, *Nanoscale*, 2018, **10**, 69–75.

76 G. Choi, F. Shahzad, Y. M. Bahk, Y. M. Jhon, H. Park, M. Alhabeb, B. Anasori, D. S. Kim, C. M. Koo and Y. Gogotsi, Enhanced terahertz shielding of MXenes with nano-metamaterials, *Adv. Opt. Mater.*, 2018, **6**, 1701076.

77 K. Li, T. H. Chang, Z. Li, H. Yang, F. Fu, T. Li, J. S. Ho and P. Y. Chen, Biomimetic MXene textures with enhanced light-to-heat conversion for solar steam generation and wearable thermal management, *Adv. Energy Mater.*, 2019, **9**, 1901687.

78 Z. Huang, X. Cui, S. Li, J. Wei, P. Li, Y. Wang and C.-S. Lee, Two-dimensional MXene-based materials for photothermal therapy, *Nanophotonics*, 2020, **9**, 2233–2249.

79 K.-T. Lin, H. Lin, T. Yang and B. Jia, Structured graphene metamaterial selective absorbers for high efficiency and omnidirectional solar thermal energy conversion, *Nat. Commun.*, 2020, **11**, 1–10.

80 L. Zhang, R. Li, B. Tang and P. Wang, Solar-thermal conversion and thermal energy storage of graphene foam-based composites, *Nanoscale*, 2016, **8**, 14600–14607.

81 B. Zhang, Y. Wang, J. Liu and G. Zhai, Recent developments of phototherapy based on graphene family nanomaterials, *Curr. Med. Chem.*, 2017, **24**, 268–291.

82 J. Li, Z. Li, X. Liu, C. Li, Y. Zheng, K. W. K. Yeung, Z. Cui, Y. Liang, S. Zhu and W. Hu, Interfacial engineering of $Bi_2S_3/Ti_3C_2T_x$ MXene based on work function for rapid photo-excited bacteria-killing, *Nat. Commun.*, 2021, **12**, 1–10.

83 Z. Guo, J. Zhou, L. Zhu and Z. Sun, MXene: a promising photocatalyst for water splitting, *J. Mater. Chem. A*, 2016, **4**, 11446–11452.

84 Z. M. Wong, T. L. Tan, S.-W. Yang and G. Q. Xu, Enhancing the photocatalytic performance of MXenes via stoichiometry engineering of their electronic and optical properties, *ACS Appl. Mater. Interfaces*, 2018, **10**, 39879–39889.

85 J. Ran, G. Gao, F.-T. Li, T.-Y. Ma, A. Du and S.-Z. Qiao, Ti_3C_2 MXene co-catalyst on metal sulfide photo-absorbers for enhanced visible-light photocatalytic hydrogen production, *Nat. Commun.*, 2017, **8**, 1–10.

86 J. Low, L. Zhang, T. Tong, B. Shen and J. Yu, TiO_2/MXene Ti_3C_2 composite with excellent photocatalytic CO_2 reduction activity, *J. Catal.*, 2018, **361**, 255–266.

87 J. Albero, D. Mateo and H. García, Graphene-based materials as efficient photocatalysts for water splitting, *Molecules*, 2019, **24**, 906.

88 J. Liu, H. B. Zhang, R. Sun, Y. Liu, Z. Liu, A. Zhou and Z. Z. Yu, Hydrophobic, flexible, and lightweight MXene foams for high-performance electromagnetic-interference shielding, *Adv. Mater.*, 2017, **29**, 1702367.

89 Z. Lin, J. Liu, W. Peng, Y. Zhu, Y. Zhao, K. Jiang, M. Peng and Y. Tan, Highly Stable 3D $Ti_3C_2T_x$ MXene-Based Foam Architectures toward High-Performance Terahertz Radiation Shielding, *ACS Nano*, 2020, **14**, 2109–2117.

90 X. Wu, B. Han, H.-B. Zhang, X. Xie, T. Tu, Y. Zhang, Y. Dai, R. Yang and Z.-Z. Yu, Compressible, durable and conductive polydimethylsiloxane-coated MXene foams for high-performance electromagnetic interference shielding, *Chem. Eng. J.*, 2020, **381**, 122622.

91 W. Ma, H. Chen, S. Hou, Z. Huang, Y. Huang, S. Xu, F. Fan and Y. Chen, Compressible highly stable 3D porous MXene/GO foam with a tunable high-performance stealth property in the terahertz band, *ACS Appl. Mater. Interfaces*, 2019, **11**, 25369–25377.

92 X. Zhao, X.-J. Zha, J.-H. Pu, L. Bai, R.-Y. Bao, Z.-Y. Liu, M.-B. Yang and W. Yang, Macroporous three-dimensional MXene architectures for highly efficient solar steam generation, *J. Mater. Chem. A*, 2019, **7**, 10446–10455.

93 H. Yin, L. Bi, Z. Wu, G. Wang, M. Li, X. Zhou, S. Ji, W. Zhang, Y. Peng and J. Pan, 2D foaming of ultrathin MXene sheets with highly conductive silver nanowires for wearable electromagnetic interference shielding applications owing to multiple reflections within created free space, *Nano Futures*, 2020, **4**, 035002.

94 X. Jia, B. Shen, L. Zhang and W. Zheng, Construction of compressible Polymer/MXene composite foams for high-performance absorption-dominated electromagnetic shielding with ultra-low reflectivity, *Carbon*, 2021, **173**, 932–940.

95 Q.-S. Rao, S.-Y. Liao, X.-W. Huang, Y.-Z. Li, Y.-D. Liu and Y.-G. Min, Assembly of MXene/PP Separator and Its Enhancement for Ni-Rich LiNi0. 8Co0. 1Mn0. 1O2 Electrochemical Performance, *Polymers*, 2020, **12**, 2192.

96 S. Bhattacharjee, R. Joshi, A. A. Chughtai and C. R. Macintyre, Graphene modified multifunctional personal protective clothing, *Adv. Mater. Interfaces*, 2019, **6**, 1900622.

97 W. Yang, J. Yang, J. J. Byun, F. P. Moissinac, J. Xu, S. J. Haigh, M. Domingos, M. A. Bissett, R. A. Dryfe and S. Barg, 3D Printing of Freestanding MXene Architectures for Current-Collector-Free Supercapacitors, *Adv. Mater.*, 2019, **31**, 1902725.

98 J. Orangi, F. Hamade, V. A. Davis and M. Beidaghi, 3D Printing of Additive-Free 2D $Ti_3C_2T_x$ (MXene) Ink for Fabrication of Micro-Supercapacitors with Ultra-High Energy Densities, *ACS Nano*, 2019, **14**, 640–650.

99 Z. Fan, C. Wei, L. Yu, Z. Xia, J. Cai, Z. Tian, G. Zou, S. X. Dou and J. Sun, 3D Printing of Porous Nitrogen-Doped Ti3C2 MXene Scaffolds for High-Performance Sodium-Ion Hybrid Capacitors, *ACS Nano*, 2020, **14**, 867–876.

100 X. Peng, Y. Zhang, D. Lu, Y. Guo and S. Guo, Ultrathin Ti3C2 nanosheets based ''off-on'' fluorescent nanoprobe for rapid and sensitive detection of HPV infection, *Sens. Actuators, B*, 2019, **286**, 222–229.

101 P. K. Kalambate, N. S. Gadhari, X. Li, Z. Rao, S. T. Navale, Y. Shen, V. R. Patil and Y. Huang, Recent advances in MXene–based electrochemical sensors and biosensors, *TrAC, Trends Anal. Chem.*, 2019, **120**, 115643.

102 J. Liu, X. Jiang, R. Zhang, Y. Zhang, L. Wu, W. Lu, J. Li, Y. Li and H. Zhang, MXene-Enabled Electrochemical Microfluidic Biosensor: Applications toward Multicomponent Continuous Monitoring in Whole Blood, *Adv. Funct. Mater.*, 2019, **29**, 1807326.

103 J. Yoon, M. Shin, J. Lim, J.-Y. Lee and J.-W. Choi, Recent Advances in MXene Nanocomposite-Based Biosensors, *Biosensors*, 2020, **10**, 185.

104 G. K. Nasrallah, M. Al-Asmakh, K. Rasool and K. A. Mahmoud, Ecotoxicological assessment of $Ti_3C_2T_x$ (MXene) using a zebrafish embryo model, *Environ. Sci.: Nano*, 2018, **5**, 1002–1011.

105 X. Han, J. Huang, H. Lin, Z. Wang, P. Li and Y. Chen, 2D ultrathin MXene-based drug-delivery nanoplatform for synergistic photothermal ablation and chemotherapy of cancer, *Adv. Healthcare Mater.*, 2018, **7**, 1701394.

106 C. Dai, H. Lin, G. Xu, Z. Liu, R. Wu and Y. Chen, Biocompatible 2D titanium carbide (MXenes) composite nanosheets for pH-responsive MRI-guided tumor hyperthermia, *Chem. Mater.*, 2017, **29**, 8637–8652.

107 H. Lin, Y. Wang, S. Gao, Y. Chen and J. Shi, Theranostic 2D tantalum carbide (MXene), *Adv. Mater.*, 2018, **30**, 1703284.

108 H. Lin, X. Wang, L. Yu, Y. Chen and J. Shi, Two-dimensional ultrathin MXene ceramic nanosheets for photothermal conversion, *Nano Lett.*, 2017, **17**, 384–391.

109 H. Lin, S. Gao, C. Dai, Y. Chen and J. Shi, A two-dimensional biodegradable niobium carbide (MXene) for photothermal tumor eradication in NIR-I and NIR-II biowindows, *J. Am. Chem. Soc.*, 2017, **139**, 16235–16247.